30
12-8-88

SLAC – PUB – 4709
October 1988
(T/E)

THE SPECTROSCOPY OF MESONS CONTAINING STRANGE QUARKS*

D. Aston,[1] N. Awaji,[2] T. Bienz,[1] F. Bird,[1] J. D'Amore,[3]
W. Dunwoodie,[1] R. Endorf,[3] K. Fujii,[2] H. Hayashii,[2] S. Iwata,[2]
W.B. Johnson,[1] R. Kajikawa,[2] P. Kunz,[1] D.W.G.S. Leith,[1] L. Levinson,[1]
T. Matsui,[2] B.T. Meadows,[3] A. Miyamoto,[2] M. Nussbaum,[3] H. Ozaki,[2]
C.O. Pak,[2] B.N. Ratcliff,[1] D. Schultz,[1] S. Shapiro,[1] T. Shimomura,[2]
P. K. Sinervo,[1] A. Sugiyama,[2] S. Suzuki,[2] G. Tarnopolsky,[1]
T. Tauchi,[2] N. Toge,[1] K. Ukai,[4] A. Waite,[1] S. Williams[1]

[1] *Stanford Linear Accelerator Center, Stanford University, Stanford, CA 94305*
[2] *Nagoya University, Furo-cho, Chikusa-ku, Nagoya 464, Japan*
[3] *University of Cincinnati, Cincinnati, Ohio 45221*
Institute for Nuclear Study, University of Tokyo, Midori-cho, Tanashi, Tokyo 188, Japan

ABSTRACT

Recent results from a high statistics study with LASS of mesons which contain strange quarks are reviewed, and compared with the quark model.

INTRODUCTION

The spectroscopy of light quark mesons continues to be an important area of investigation in high energy physics. Historically, it was of vital importance to the early success of the quark model, and it is now well-known that the non-relativistic quark model provides an excellent description of most of the known light quark spectra, and the observed heavy quark mesons as well.[1,2] In the context of these models, studies with light quarks complement those of the heavy quarkonia in that they probe a different piece of the $q\bar{q}$ potential, and allow the study of the strength and structure of the long-range confining term of the interaction. However, none of the meson spectra is well mapped over most of the excitation space, and, since the experimentally accessible states depend strongly on the production mechanism, studies of both light and heavy mesons in a wide variety of channels remain of interest. In particular, the discovery of several candidates for exotic mesons in the mass region below 2.3 GeV/c^2, as described at this conference, emphasizes yet again the importance of understanding the $q\bar{q}$ levels in this mass region as a template against which the exotic candidates can be compared.

*Work supported in part by the Department of Energy under contract No. DE-AC03-76SF00515; the National Science Foundation under grant Nos. PHY82-09144, PHY85-13808, and the Japan U.S. Cooperative Research Project on High Energy Physics.

Invited talk presented by B. Ratcliff at the BNL Workshop on Glueballs, Hybrids, and Exotic Hadrons, Brookhaven National Lab. Upton, NY, August 29-September 1, 1988

SLAC-PUB--4709

DE89 003786

CONF-8808102--4

THE EXPERIMENT

This talk reviews several recent results on mesons containing strange quarks coming from the LASS collaboration at SLAC. Details of these analyses can be found elsewhere.[3,4,5,6,7,8,9] The spectrometer is serviced by a clean RF separated beam, and has nearly flat acceptance over 4π steradians, good particle identification, good multi-particle tracking and topology reconstruction, a full acceptance trigger, and high data rate capability.[10] The raw data sample contains $\sim$ 113 million triggers taken with an 11 GeV/c K^- beam, corresponding to a sensitivity of 4.1 events/nb.

K^* SPECTROSCOPY

The strange mesons provide an excellent laboratory to study a pure $q\bar{q}$ system since there is no isoscalar-isovector mixing and no confusion with pure glueballs. In particular, the reactions

$$K^- p \to K^- \pi^+ n \tag{1}$$

and

$$K^- p \to \overline{K}^0 \pi^+ \pi^- n \tag{2}$$

are ideal places to study the orbital excitation ladder and also provide access to the expected underlying states. Reaction (1) has a particularly simple topology, is restricted to the natural spin-parity series, and has a large cross section which is dominated by π exchange at small values of momentum transfer ($t' \equiv |t - t_{min}|$), whereas reaction (2) can couple to both natural and unnatural spin-parities. I will only discuss features of a few of the natural spin-parity objects in the following section. Many more details of these analyses are given elsewhere.[3,4]

The invariant mass distribution for reaction (1) is shown in fig. 1 for the 730,000 events with $t' \leq 1.0$ GeV/c^2. The spin-parity $J^P = 1^- K^*(892)$ and $2^+ K_2^*(1430)$ mesons can be clearly seen as can a higher mass structure in the $3^- K_3^*(1780)$ region. Similarly, the invariant mass for reaction (2) shown in fig. 2 has structure in the $K_2^*(1430)$ and $K_3^*(1780)$ regions. However, in neither case is there any direct evidence in the mass plots for the higher mass leading resonances nor for the expected underlying states, and at first sight the cross sections appear to be largely background on which the low mass leading resonances are superimposed.

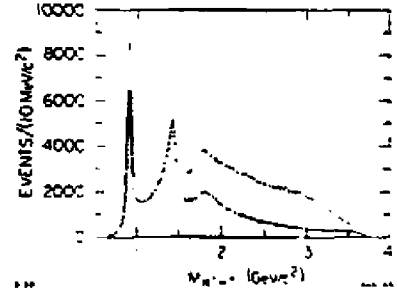

Fig. 1. The $K^-\pi^+$ mass distribution from reaction (1); the cross-hatched plot contains events with N^*'s removed ($M(n\pi^+) \geq 1.7$ GeV/c^2).

Partial wave analyses (PWA) of these data show, however, that the cross sections are composed of many resonances; indeed, even the "obvious" leading structures contain significant contributions from underlying resonances in the same mass regions.

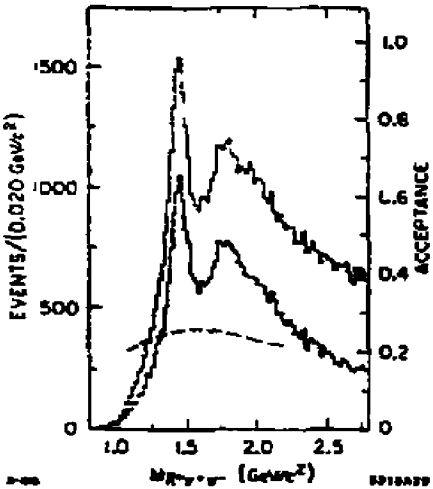

Fig. 2. The $K^0_S\pi^+\pi^-$ mass distribution from reaction (2) for all events (top plot) and for events with $t' \leq 0.3$ GeV/c^2 (bottom plot); the dashed line gives the final acceptance after all cuts.

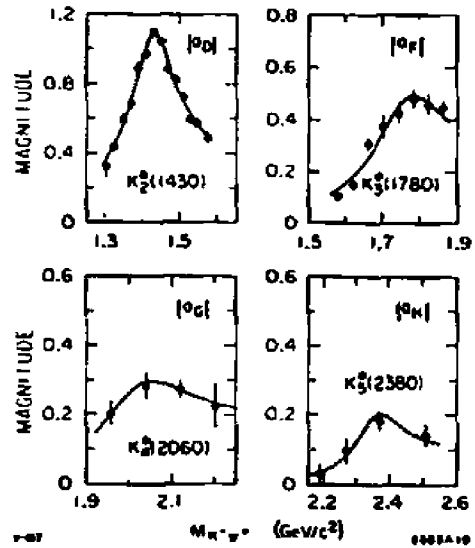

Fig. 3. The leading natural spin-parity resonant amplitudes from reaction (1).

The PWA amplitudes for reaction (1) demonstrate clear Breit-Wigner structures for the leading orbitally excited natural spin-parity states with J^P from 2^+ up to 5^-, as shown in fig. 3. The $K_2^*(1430)$, the $K_3^*(1780)$, the $K_4^*(2060)$, and the $K_5^*(2380)$ are clearly seen. Similarly, the same leading natural spin-parity resonances with J^P up to 4^+ can be seen in the natural spin-parity waves of reaction (2), as shown in fig. 4. There is also substantial structure in the 1^- wave around 1.4 and 1.8 GeV/c^2, and in the 2^+ wave around 2.0 GeV/c^2. The individual K^* and ρ isobar contributions to the 1^- wave in reaction (2) are shown in fig. 5, and, as shown by the curves, these waves are well described by a model with two 1^- Breit–Wigner resonances. The higher mass state, with $M=1735 = 10 \pm 20$ and $\Gamma = 423 \pm 18 = 30$, couples to both channels; while the lower mass state, with $M=1420 \pm 7 \pm 10$ and $\Gamma = 240 \pm 18 \pm 12$, is nearly decoupled from the $K\rho$ channel, and its production characteristics suggest a weak $K\pi$ coupling as well. This behavior is corroborated by the P wave $K\pi$ amplitude shown in fig. 6, which has clear resonances around 890 and 1700 MeV/c^2, but a model incorporating only these two resonances is incapable of describing the data in the 1400 Mev/c^2 region as is indicated by the dashed line. However, the three resonance model shown by the solid line provides a good description of the data in terms of the $K^*(892)$, a resonance at $M=1380 \pm 21 \pm 19$ MeV/c^2 with an elasticity of 0.07, and a third resonance at $M=1677 \pm 10 \pm 32$ with an elasticity of 0.39, in good agreement with the characteristics of the states seen in reaction (2).

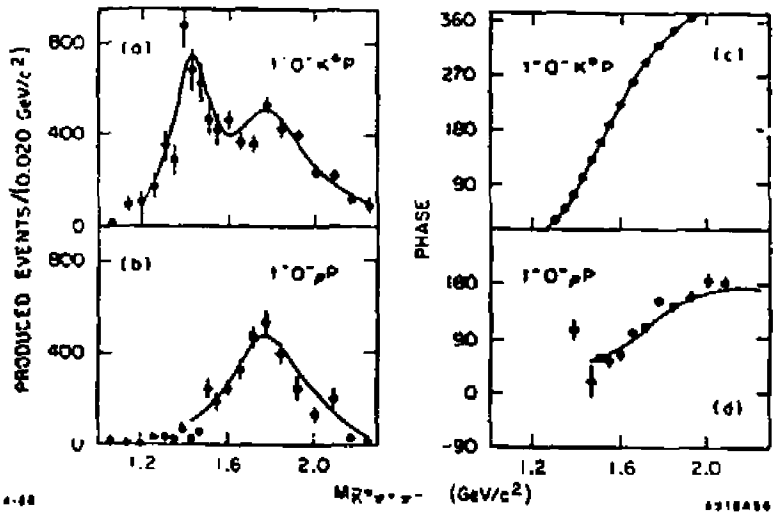

Fig. 4. The natural spin-parity wave sums from reaction (2).

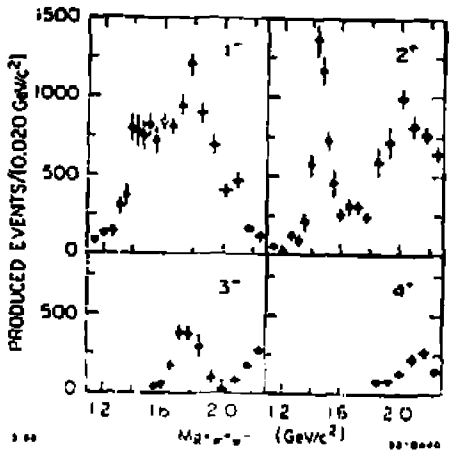

Fig. 5. The individual isobar contributions to the 1^- wave from reaction (2).

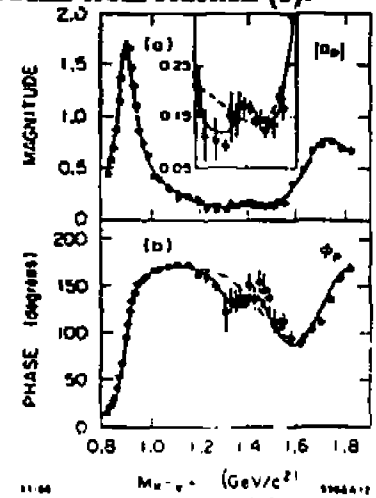

Fig. 6. The intensity (a) and phase (b) of the P wave $K\pi$ amplitude from reaction (1) below 1.84 GeV/c^2.

It is simplest to associate the higher state with the 1^3D_1 state based on the small triplet splitting and the agreement of the branching ratios with SU(3). Though mixing is not excluded, the lower state then would be mostly the first radial excitation of the $K^*(892)$. The suppression of the $K\pi$ decay mode of the lower mass state is understood in some models as being a dynamical effect resulting from the presence of a node in the radial wave function.[11]

The PWA of reaction (1) also provides clear evidence for two structures in the S wave. The first, which can be seen at around 1.4 GeV/c^2 in fig. 7, is generally classified as the $^3P_0$ triplet partner of $K_2^*(1430)$, and has been seen by

several earlier experiments.[3] Determination of its resonance parameters is complicated by the large elastic phase shift in the low mass region and the proximity of $K\eta'$ threshold, and the parameters are therefore quite model dependent. The fit shown by the line in the figure uses the model developed by Estabrooks[12] giving the values M=1412 $\pm$ 1 MeV/c^2, $\Gamma = 294 \pm 4$, and elasticity $\epsilon = 1.0 \pm 0.05$, where the errors are statistical only. On other hand, the phase shift reaches 90° at ~ 1340, and other models suggest that the resonance mass lies close to this point.[3]

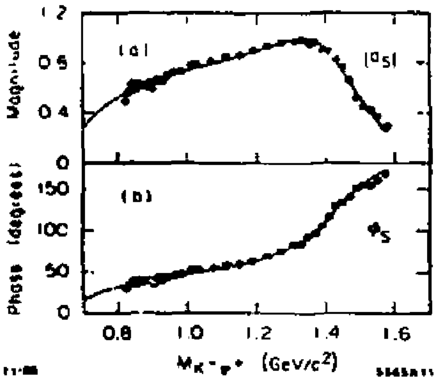

Fig. 7. The intensity and phase of the $I = 1/2$ S wave amplitude from reaction (1) below 1.6 GeV/c^2.

There is a second S wave structure at around 1.9 GeV/c^2 shown in fig. 8. Though there are two solutions in this mass region, they both show resonance behavior with approximate parameters M~ 1950, $\Gamma \sim 200$ MeV/c^2, and $\epsilon \sim 0.5$. Within the quark model, this state can only be classified as a radial excitation of the 0^+ member of the L=1 triplet, most probably the 2^3P_0 state. The 2^+ wave from reaction (2) also demonstrates resonance behavior in this same mass region (M=1973 $\pm$ 33 MeV/c^2, Γ = 373$\pm$93), which most probably is the radial excitation of the $K_2^*(1430)$ and the triplet partner of the 0^+ state.

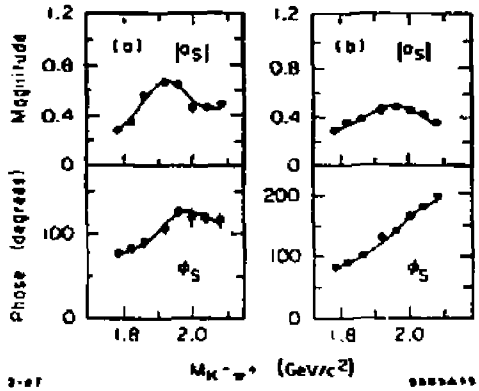

Fig. 8. The intensity and phase of the S wave amplitude from reaction (1) for the two solutions, (a) and (b), in the mass region between 1.76 and 2.14 GeV/c^2.

The reaction

$$K^-p \to K^-\eta\, p \ ; \tag{3}$$

is particularly interesting since SU(3) makes the striking prediction that the $K\eta$ branching ratios from even-spin K^* states will be very small, while those of odd-spin states should be substantial. The $K\eta$ mass spectrum of fig. 9(a), and the results of the PWA shown in fig. 9(b) demonstrate that this prediction is indeed correct. Production of the $K_3^*(1780)$ is seen clearly with a branching fraction to $K\eta$ of 7.9 $\pm$ 2.4%, while the 95% confidence level upper limit on the $K\eta$ branching fraction of the $K_2^*(1430)$ is measured to be 0.45%.

Figure 10 summarizes the K^* spectrum observed from this experiment in the channels discussed today. The observed leading states lie on an essentially linear orbital ladder that extends up through the 5^- K^*. Several of the expected triplet multiplets have now been seen and there are good candidates for radial

states. In general, the parameters of these states agree well with the predictions of the quark model,[1] with some exceptions which are discussed in the concluding section. We have measured π transitions from most of these states as well as transitions to vector, and in some cases, tensor and η mesons, and, in general, the decay rates are consistent with those predicted by SU(3).

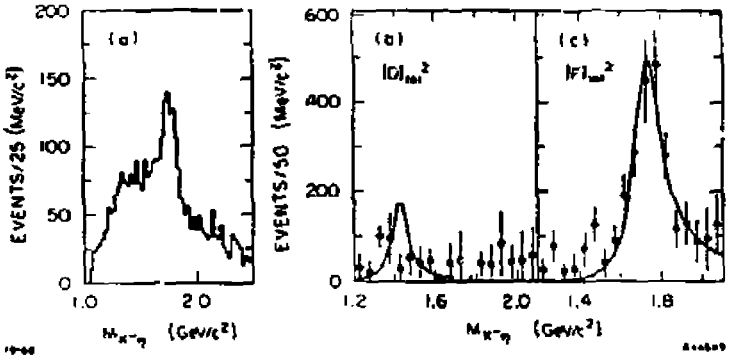

Fig. 9. The $K\eta$ mass dependences from reaction (3) for: (a) the raw data with $M(\eta p) \geq 2.0$ GeV/c^2 and $M(K^-p) \geq 1.85$GeV/c^2; (b) the intensity distributions for D and F waves; the Breit-Wigner curve on the D wave indicates the 95% c.l. limit for $K_2^*(1430)$ production, while the curve on the F wave indicates the Breit-Wigner fit to the $K_3^*(1780)$.

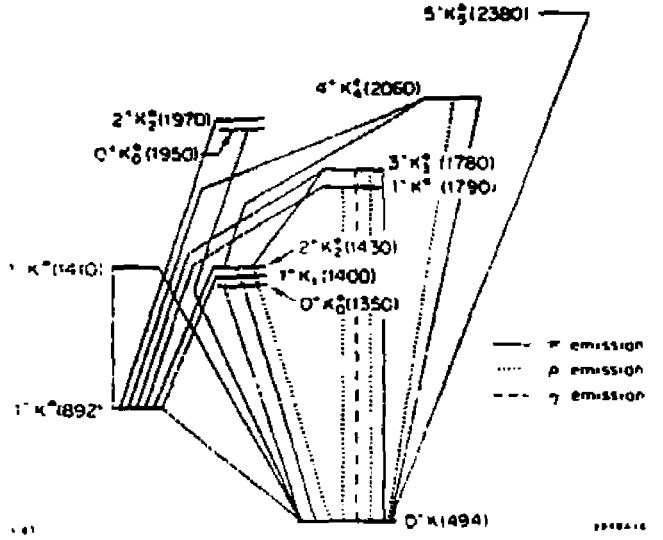

Fig. 10. Level diagram summarizing the strange meson states and transitions seen in this experiment.

$s\bar{s}$ SPECTROSCOPY

The strangeonium mesons are of particular interest since several candidates for exotic mesons, as discussed at this conference, couple strongly to the same final states. The reactions

$$K^- p \to K^- K^+ \Lambda \tag{4}$$

$$K^- p \to K^0_S K^0_S \Lambda \tag{5}$$

$$K^- p \to K^0_S K^\pm \pi^\mp \Lambda \tag{6}$$

are dominated by peripheral hypercharge exchange which strongly favors the production of $s\bar{s}$ mesons over glueballs. Thus, these channels provide a clear look at the strangeonia, which can provide revealing comparisons with the same final states produced in other channels that might be glue-enriched. Only a very short review of the material of direct relevance to $s\bar{s}$ spectroscopy is given here. More details were given to this conference in the talk of D. Aston, and in published papers.[6,7,8,9]

The mass spectrum of fig. 11(a) for reaction (4) shows bumps corresponding to the known $\phi(1020)$ and $f_2'(1525)$ leading orbital states as well as a smaller bump in the $\phi_J(1850)$ region. Only the $f_2'(1525)$ is observed in fig. 11(b) for reaction (5) since it is restricted to even spin states. In neither case is there any evidence for the $\theta(1720)$. Amplitude analyses of these data (fig. 12) display the expected P wave structure for the $\phi(1020)$ and D wave for the $f_2'(1525)$. In addition, the S wave intensity [fig. 12(d)] from reaction (5) appears to peak around the $f_2'(1525)$ mass. Although the errors on the individual points are large (and non-linear), the data require the existence of an S wave in this region at about the 5σ level. This suggests the existence of a 0^+ resonance which is most naturally interpreted as the triplet partner of the $f_2'(1525)$,[6] and leads us to suggest that the $f_0(975)$, which is usually assigned to this multiplet, may not be a $q\bar{q}$ state.

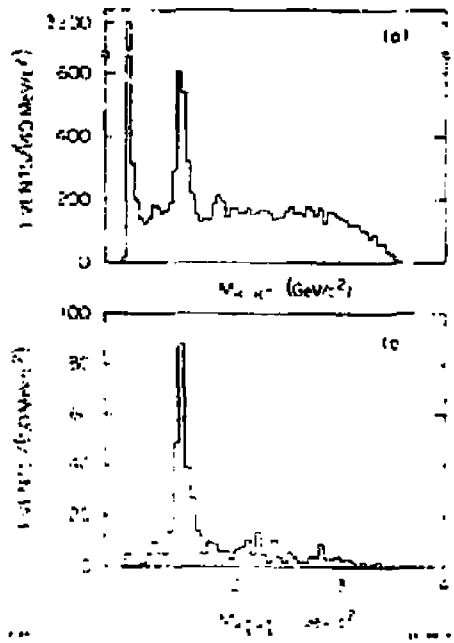

Fig. 11. The $K\bar{K}$ mass spectra from (a) reaction (4); and (b) reaction (5).

The F wave intensity distribution of fig. 13(a) shows a structure in the 1850 MeV/c^2 region which can be simply associated with the $\phi_J(1850)$ bump in the mass distribution [fig. 13(b)]. A Breit-Wigner fit to the F wave amplitude of fig. 13(a) gives parameters $M = 1855 \pm 22$, $\Gamma = 74 \pm 67$ MeV/c^2, while a fit

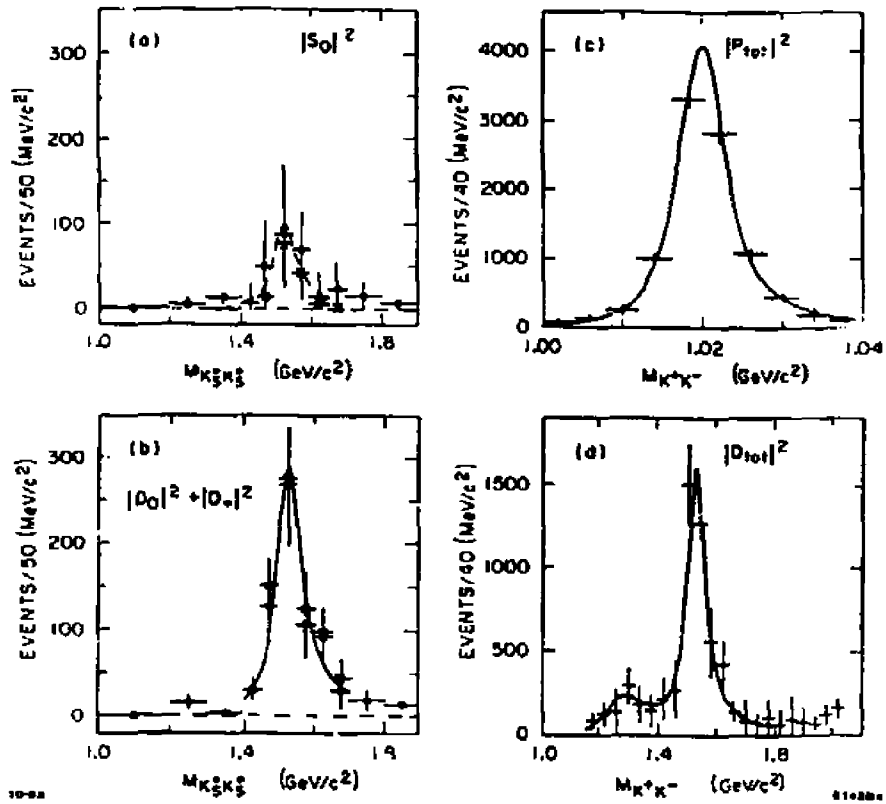

Fig. 12. The low mass $K\bar{K}$ amplitudes from: (a-b) reaction (5); (c-d) reaction (4).

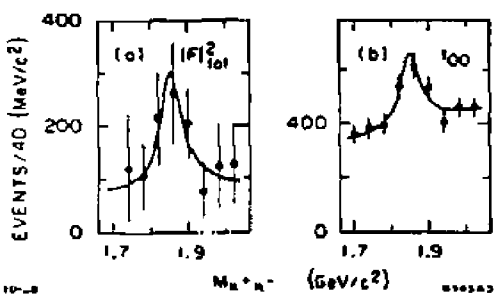

Fig. 13. The mass region around 1850 MeV/c^2 from reaction (4); (a) the F wave intensity; (b) the mass dependent total cross section.

to the cross section gives M=1851 ± 7, Γ = 66 ± 29 MeV/c^2. We have also shown that the interference between $s\bar{s}$ resonance production and diffractive N^* production can be utilized to analyze the leading the $s\bar{s}$ amplitude, and this method gives results consistent with the above for the F wave.[8] An extension of this method has been utilized to analyze the G wave amplitude in the 2.2 GeV/c^2 mass region. Fig. 14 shows evidence for a 4^+ state (the $f_4'(2210)$ which is a good candidate to be the mainly $s\bar{s}$ member of the 4^{++} nonet predicted by the quark model.

The most prominent features of the $K\bar{K}\pi$ mass distribution [fig. 15(a)] from reaction (6) are a sharp rise at $K^*\bar{K}$ threshold followed by a peak around 1.5 GeV/c^2, and a second peak around 1.85 GeV/c^2. The PWA shows that the low mass region is dominated by 1^+ K^* waves, while the higher mass structure contains evidence for peaks in the 2^- and 3^- waves. The 1^+ waves can be combined to form eigenstates of G-parity as shown in fig. 15(b) and 15(c). These distributions are well described by Breit-Wigner curves as shown, and, assuming $I = 0$, provide good evidence for two $s\bar{s}$ axial-vector meson states: one with quantum numbers $J^{PC} = 1^{++}$, M~ 1530 MeV/c^2, and $\Gamma \sim 100$ MeV/c^2, and the other with $J^{PC} = 1^{+-}$, M~ 1380 MeV/c^2, and $\Gamma \sim 80$ MeV/c^2. These states are good candidates to be the mostly strangeonium members of the ground state 1^{++} and 1^{+-} nonets predicted by the quark model.

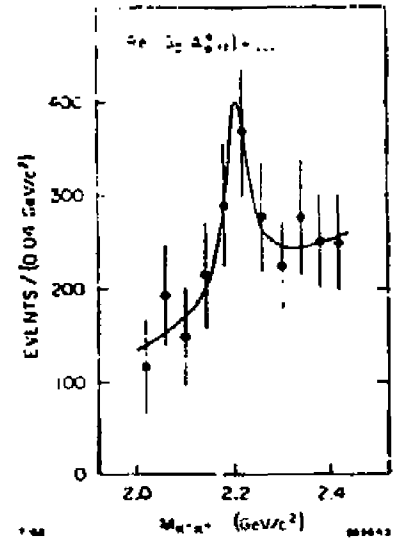

Fig. 14. The mass dependence of the interference between the G_0 and diffractive background amplitudes from reaction (4).

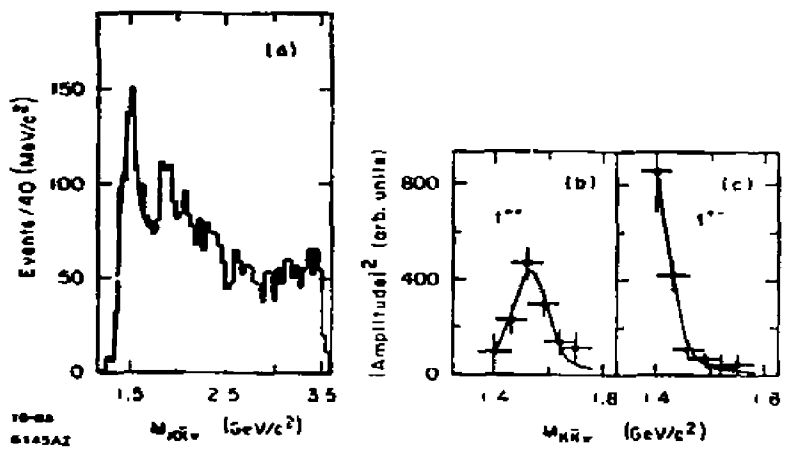

Fig. 15. The $K\bar{K}\pi$ mass distribution (a) from reaction (6); (b-c) the 1^+ G-parity eigenstate amplitudes

Fig. 16 summarizes the strangeonia observed from this experiment in the channels discussed today. The general features of the spectrum are reminiscent of the K^* spectrum discussed above. The observed leading states lie on an essentially linear orbital ladder that extends up through the 4^+ f_4', and there are good candidates for the triplet partners of the $f_2'(1525)$. Except for the ground state pseudoscalar, the states appear to fit into SU(3) multiplets which are consistent with magic mixing, and the parameters and decay transitions of these states agree well with the predictions of the quark model.[1,13]

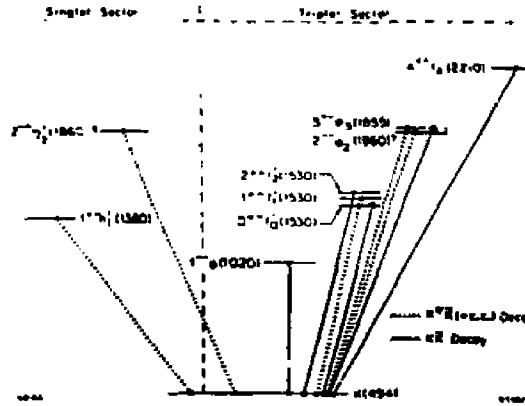

Fig. 16. Level diagram summarizing the strangeonium meson states and transitions seen in this experiment.

CONCLUSION

The more that is learned about the light $q\bar{q}$ spectra, the simpler and more pronounced the experimental regularities seem to be. An optimistic reading of those regularities from the data reviewed here leads to the suggestion made by Isgur at this conference that the spectra are "too" simple, and fit the nonrelativistic quark model extremely well. In particular, the many states seen here fit naturally into the predicted $q\bar{q}$ levels, with orbital excitations lying on linear trajectories and rather small triplet $(L \cdot S)$ splittings. The flavor dependences between spectra are also very simple, and, except for the ground states, the singlet-triplet splittings seem small and the nonets are approximately magically mixed. Moreover, $SU(3)$ predicts most of the decay rates well, and the production processes are fairly well understood.

Yet, important questions remain. First, it must be recognized that few triplet or singlet-triplet splittings are well measured, and many of the high mass orbital states have large errors on their masses, so that many of the detailed systematics indicated by these data need substantially more study. Second, there are a number of indications that all is not well with the optimistic picture of the $q\bar{q}$ system painted above. In particular, the 2^3S_1 $K^*(1410)$ seems to lie much lower in mass than simple predictions would indicate, and its small coupling to $K\pi$ indicates a breakdown in the simple SU(3) model of decay rates, perhaps pointing to a need to include radial wavefunction dynamics in the models. Finally, with the rather complete picture of the low mass $q\bar{q}$ systems as given here, it is becoming increasingly clear that several states seen primarily in other production modes have no convenient home in the $q\bar{q}$ sector. For example, low mass 0^{++} systems have been confusing for many years, and it now seems quite clear that there are "too many" such states. Moreover, as has been extensively discussed at this conference, the E/ι and $\theta(1720)$ regions contain many puzzles. These observations point to the existence of meson physics beyond the quark model and lead to the hope that these new spectroscopies soon will emerge more clearly.

REFERENCES

1. see, for example, S. Godfrey and N. Isgur, Phys. Rev. D32(1985) 189.
2. Particle Data Group, Phys. Lett. 170B (1986).
3. D. Aston et al., Nucl. Phys. B292(1987) 693.
4. D. Aston et al., Phys. Lett. 180B(1986) 308; Nucl. Phys. B296(1988) 493.
5. D. Aston et al., Phys. Lett. 201B(1988) 169.
6. D. Aston et al., Nucl. Phys. B301(1989) 525.
7. D. Aston et al., Phys. Lett. 201B(1988) 573.
8. D. Aston et al., Phys. Lett. 208B(1988) 324.
9. D. Aston et al., DPNU-88-24 / SLAC-PUB-4661 (1988).
10. D. Aston et al., The LASS Spectrometer, SLAC-REP-298 (1986).
11. see for example, A. Bradley, J. Phys., G4(1978) 1517.
12. P. Estabrooks, Phys. Rev., D19(1979) 2678.
13. S. Godfrey and N. Isgur, Phys. Lett. 141B(1984) 439.

DISCLAIMER